Journal of Applied Mathematics and Physics, 2023, 11, 582-597
https://www.scirp.org/journal/jamp
ISSN Online: 2327-4379
ISSN Print: 2327-4352

Polarization Simultons in CARS by Polaritons

Vladimir Feshchenko[1], Galina Feshchenko[2]

[1]Dawson College, Montreal, Canada
[2]Vanier College, Montreal, Canada
Email: vfeshchenko@dawsoncollege.qc.ca, feshcheg@vaniercollege.qc.ca

How to cite this paper: Feshchenko, V. and Feshchenko, G. (2023) Polarization Simultons in CARS by Polaritons. *Journal of Applied Mathematics and Physics*, **11**, 582-597.
https://doi.org/10.4236/jamp.2023.112036

Received: November 9, 2022
Accepted: February 25, 2023
Published: February 28, 2023

Abstract

The system of shortened Maxwell's equations simulating the processes of evolution of the stimulated Raman scattering (SRS) by polaritons in anisotropic dipole-active crystals is obtained. The theory was developed for the case of cubic crystals which become anisotropic due to the deformation of the dielectric constant by the linearly polarized pump wave. The pump field is a linearly polarized plane electromagnetic wave. We report the results of the theoretical investigation of the possibility of the existence of a regime of pulse propagation as simultaneous travel of solitary waves in coherent anti-Stokes stimulated Raman scattering by polaritons in anisotropic crystals. The emphasis was made on the existence of both Stokes and anti-Stokes pulses propagating with two stable and perpendicular to the direction of travel polarizations. We showed the theoretical possibility of simultaneous propagation of pulses not only at frequencies of Stokes and anti-Stokes waves but the pump frequency as well. We obtained the expression for the gain factor g. It is also shown that the expression for g is consistent with the experimental results for the spectra of ZnS.

Keywords

Nonstationary Stimulated Raman Scattering, Polaritons, Phonons, Solitons, Polarization

1. Introduction

Past decades showed significant progress in both theory of solitons and their multiple applications. The theoretical consideration includes, for instance, considering 3D solitons [1], solitons in exciton-polariton condensates [2], solitons of phonon polaritons and plasmon-polariton [3], solitons in multi-photonic processes [4], dissipative solitons [5] [6], Raman solitons in structures with metamaterials [7], solitons in SRS [8], etc. We also see the tremendous success in applying solitons in new substances whose characteristics could improve the properties of optical communication systems [9] [10] [11] [12] [13]. In [9] a new almost dispersionless mode in the photonic band gap in $LiNbO_3$ is obtained. The article [10] reports experimental results on phonon-polariton Raman scattering in a hexagonally poled $LiTaO_3$ crystal, showing that the anti-Stokes and Stokes Raman intensities are significantly enhanced by cascading a couple of quasi-phase-matching processes where the coherent polariton fields are driven and the enhanced scattering signals are further amplified. The demonstration of the distortion-free propagation of polariton pulses in CuCl is considered in [11]. The effects of the exciton dispersion on the properties of polariton solitons in gyrotropic and non-gyrotropic crystals are investigated in [12]. The first observation of spontaneous Raman solitons in Raman scattering by the NH_3 is reported in [13]. Significant progress is achieved in developing waveguides (see, for example [14] [15] [16]). In [14] was demonstrated that the giant nonlinearity of UV hybrid light-matter states (exciton-polaritons) up to room temperature, would lead to a new generation of integrated UV nonlinear light sources for advanced spectroscopy and measurement. The theoretical study of the magneto-optical manipulation of surface polaritons (SP_s) in the negative index metamaterial-dielectric interface waveguide system leading toward the creation of optical logic gates is shown in [15]. The analysis of the influence of Raman-induced self-frequency shift in two-component solitons, supported by both quadratic and cubic nonlinearities on soliton stability is reported in [16]. We also see new developments in the theory and application of microcavities and microcavity lasers [17]-[23]. In [17] we find the reported results of studying the nonstationary nonlinear processes in the lithium-niobite-on insulator (LiNOI) platform, which offers both large quadratic and cubic nonlinearities thus enabling brand new nonlinear photonic devices and applications for the next generation of integrated photonic circuits. Detailed analysis of polariton-mediated Raman scattering in microcavities is shown in [18]. The observation of bright polariton solitons in a semiconductor microcavity is provided in [19] [20] [21]. The unique perspectives toward ultrafast nonlinear photonics by exploiting the coupling of atomic motion and solitons inside a cavity are discussed in [22]. The theoretical and experimental investigation of an easily reproducible way to generate Raman solitons with controllable spectral width in an anomalous dispersion region in a functionalized silica microsphere is discussed in [23]. Of course, we also see progress in further development in both theoretical and practical domains of optical fibers and fiber lasers using solitons [24] [25] [26]. In [24] the research is focused on the numerical study of dark solitons in normal-dispersion optical fibers described by the cubic-quintic complex Ginzburg-Landau equation with the existence of chaotic content and the tunneling through a potential barrier. The high-power intra-cavity Raman solitons within a passively mode-locked Yb-doped fiber laser were demonstrated successfully for the first time in [25]. The results of tunable mid-infrared Raman soliton generation in an all-solid fluoro-tellurite fiber pumped by a 1960 nm femtosecond fiber laser are in [26].

The important feature of an optical pulse along with the amplitude and frequency is its polarization. It is very desirable to have solitons with certain polarization since this feature can be used for the delivery of additional information in communication systems. Such analysis for microcavity lasers is presented in [27] [28] [29]. The authors of [27] reported the results obtained for the state of polarization in the emission of a vertical-cavity surface-emitting laser with frequency-selective feedback added. The influence of polarization on the formation of vectorial polariton in semiconductor microcavities through numerical simulations is considered in [28]. In the case of optical fibers, since they are randomly birefringent and solitons formatting and traveling in them are randomly polarized, it is desirable to have solitons with a well-defined polarization [29]-[43]. The theoretical and experimental study of soliton propagation in fiber lasers and its relationship with polarization is discussed in [44] [45] [46]. For example, [44] reports on the experimental observation of two types of a phase-locked vector soliton in weakly birefringent cavity erbium-doped fiber lasers. The results of the study of the polarization dynamics of ultrafast solitons in mode-locked lasers are presented in [45]. The vector feature of the dissipative solitons formed in a fiber laser is investigated in [46].

On the other hand, since optoelectronic systems have a large bandwidth, it would be promising to have several temporal solitons, traveling through the medium simultaneously. Some theoretical aspects of such propagation (different substances, different mechanisms, etc.) were considered in [47] [48] [49]. The generation of three-wave solitons in the resonant LO-phonon-mediated interaction of two intense coherent polaritons is proposed in [47]. We considered the theory and computer simulation of simultons formation in stimulated Roman scattering by polaritons in dipole-active crystals [48] [49]. In past years progress was also achieved in the process of the realization of solitons at different frequencies [50] [51] [52]. The study of a compact nanotube-mode-locked all-fiber laser that can simultaneously generate picosecond and femtosecond solitons at different wavelengths is considered in [50]. The numerical and experimental investigation of the dynamics of dual-color-soliton collisions inside a mode-locked laser can be found in [51]. The experimental observation of polychromatic gap solitons generated by supercontinuum light in an array of optical waveguides, see in [52]. However, in our opinion, some aspect that could significantly broaden the diversity of soliton applications is the propagation of solitons not only having certain frequencies but definite polarizations as well. Authors think that one of the perspective applications of simultaneously propagating solitons with fixed polarizations (polarization simultons) is their application in digital systems with one polarization considered to be “zero” and another as “1”. The example of nonlinear processes leading to the formation of such polarization simultons was considered in [53], in which we studied the conditions of their formation in stimulated Raman scattering by polaritons. In the present paper, we theoretically consider a more general case: polarization soliton formation at not only Stokes frequency but anti-Stokes as well. Our theory developed for CARS in dipole-active anisotropic crystals is consistent with experimental results.

2. Basic Principles and Equations

In the present article, we consider the nonlinear interaction of four electromagnetic waves: anti-Stokes, Stokes, laser pump, and polariton. The pump wave is a linearly polarized plane electromagnetic wave whereas anti-Stokes and Stokes have two mutually perpendicular components (the nonlinear medium is assumed to be nonmagnetic and transparent at frequencies of anti-Stokes, Stokes, and laser waves). It is also assumed that the nonlinear interaction takes place in a nonlinear medium in a form of a layer bounded by the planes $z = 0$ and $z = L$. The pump wave

$$\vec{E}_l(\vec{r},t) = \hat{e}_l A_l(z,t)\exp\left[i\left(k_l^z z - \omega_l t\right)\right] + c.c. \tag{1}$$

propagates along the z-axis. The subscripts *a*, *l*, *s*, and *p* henceforth denote the anti-Stokes, laser, Stokes, and polariton waves at the frequencies $\omega_{a,l,s,p}$. We use the expressions for the anti-Stokes, Stokes, and polariton fields in the form

$$\vec{E}_a(\vec{r},t) = \sum_{\mu=1,2} \hat{e}_a^{(\mu)} A_a^{(\mu)}(z,t)\exp\left[i\left(\vec{k}_a\vec{r} - \omega_a t\right)\right] + c.c. \tag{2}$$

$$\vec{E}_s(\vec{r},t) = \sum_{\mu=1,2} \hat{e}_s^{(\mu)} A_s^{(\mu)}(z,t)\exp\left[i\left(\vec{k}_s\vec{r} - \omega_s t\right)\right] + c.c. \tag{3}$$

$$\vec{E}_p(\vec{r},t) = \sum_{\sigma=1,2,3} \hat{e}_p^{(\sigma)} A_p^{(\sigma)}(z,t)\exp\left[i\left(\vec{W}\vec{r} - \omega_p t\right)\right] + c.c. \tag{4}$$

where $k_{a,s,l,p} = q_{a,s,l,p} n_{a,s,l,p}$; $n_{a,s,l,p}$ and $k_{a,s,l,p}$ are the refractive indices and the magnitude of wave vectors in the unpumped medium; $\hat{e}_{a,s,l,p}$ are the real unit vectors of corresponding electromagnetic fields; $q_{a,s,l,p} = \omega_{a,s,l,p}/c$; $\vec{W} = \vec{k}_l - \vec{k}_s$; $\omega_p = \omega_l - \omega_s$; $\hat{e}_{a,s}^{(\mu)} \perp \vec{k}_{a,s}$, $\hat{e}_{a,s}^{(1)} \perp \hat{e}_{a,s}^{(2)}$, $\hat{e}_p^{(1,2)} \perp \vec{W}$, $\hat{e}_p^{(1)} \perp \hat{e}_p^{(2)}$, $\hat{e}_p^{(3)} = \vec{W}/W$.

Since we consider the non-resonant frequencies, the longitudinal components of the anti-Stokes and Stokes waves can be neglected, but this cannot be done for the polariton wave in the vicinity of the phonon resonance. As it was shown in [54] with a further advance towards this region the amplitudes of all three polariton waves $A_p^{(\sigma)}$ become comparable at first, then $A_p^{(3)}$ (the longitudinal component) becomes dominant (of course, if such excitation is allowed by the selection rules). The phase of the polariton wave is determined by the vector $\vec{W}$ (not by $\vec{k}_p$ ($k_p = q_p\sqrt{\varepsilon_p}$, $\varepsilon_p = \varepsilon_p' + i\varepsilon_p''$ is the dielectric constant at the polariton frequency ω_p)).

The nonlinear interaction of the electromagnetic waves $\omega_{l,s}$ with the further generation of anti-Stokes and polariton waves is described by the nonlinear parts of the corresponding polarizations ($\mu = 1,2$):

$$\begin{gathered}
P_a^{(\mu)} = \chi_a^{\mu\sigma} A_l A_p^{(\sigma)} e^{-i\Delta k^z z} + \gamma_{a2}^{\mu\mu'} \left|A_l\right|^2 A_a^{(\mu')} + \gamma_{a2}^{\mu\mu'\mu''} A_s^{(\mu)} A_s^{(\mu')} A_a^{(\mu'')} \\
P_l = \chi_{l1}^{\mu\sigma} A_s^{(\mu)} A_p^{(\sigma)} + \chi_{l2}^{\mu\sigma} A_a^{(\mu)} A_p^{(\sigma)*} e^{i\Delta k^z z} \\
P_s^{(\mu)} = \chi_s^{\mu\sigma} A_l A_p^{(\sigma)*} + \gamma_{s1}^{\mu\mu'} \left|A_l\right|^2 A_s^{(\mu')} + \gamma_{s2}^{\mu\mu'\mu''} A_a^{(\mu)} A_a^{(\mu')} A_s^{(\mu'')}
\end{gathered} \tag{5}$$

$$P_p^{(\sigma,\mu)} = \chi_{p1}^{\mu\sigma} A_l^* A_s^{(\mu)} + \chi_{p2}^{\mu\sigma} A_l A_a^{(\mu)*} \exp\left(-i\Delta k^z z\right) \quad (\sigma = 1,2)$$

$$P_p^{(3)(\mu)} = \chi_{p1}^{\mu3} A_l^* A_s^{(\mu)} + \chi_{p2}^{\mu3} A_l A_a^{(\mu)*} \exp\left(-i\Delta k^z z\right),$$

where $\chi_a^{\mu\sigma}$, $\chi_{l1}^{\mu\sigma}$, $\chi_{l2}^{\mu\sigma}$, $\chi_s^{\mu\sigma}$, $\chi_{p1}^{\mu\sigma}$, $\chi_{p2}^{\mu\sigma}$, $\chi_{p1}^{\mu3}$, $\chi_{p2}^{\mu3}$, $\gamma_{a2}^{\mu\mu'}$, $\gamma_{a2}^{\mu\mu'\mu''}$, $\gamma_{s1}^{\mu\mu'}$, and $\gamma_{s2}^{\mu\mu'\mu''}$ are the corresponding tensor contractions of the non-resonance quadratic and cubic nonlinear polarizabilities with unit vectors of interacting waves; $\Delta k^z \equiv k_l^z + W^z - k_a^z$.

The system of shortened equations for the amplitudes $A_{a,l,s,p}$ is obtained from Maxwell's equations by using the standard method of getting shortened equations by applying the approximation of slowly varying amplitudes [55]

$$\mu = 1,2, \quad \sigma = 1,2,3$$

$$\begin{aligned}&\frac{\partial A_a^{(\mu)}}{\partial z} + \frac{1}{v_a^{z(\mu)}} \frac{\partial A_a^{(\mu)}}{\partial t} \\ &= i \frac{2\pi\omega_a}{c n_a^{(\mu)} \cos\theta_a^{z(\mu)}} \left\{ \chi_a^{\mu\sigma} A_l A_p^{(\sigma)*} \mathrm{e}^{-i\Delta k^z z} + \gamma_{a2}^{\mu\mu'} \left|A_l\right|^2 A_a^{(\mu')} + \gamma_{a2}^{\mu\mu'\mu''} A_s^{(\mu)} A_s^{(\mu')*} A_a^{(\mu'')} \right\},\end{aligned} \tag{6}$$

$$\frac{\partial A_l}{\partial z} + \frac{1}{v_l^z} \frac{\partial A_l}{\partial t} = i \frac{2\pi\omega_l}{c n_l \cos\theta_l^z} \left\{ \chi_{l1}^{\mu\sigma} A_s^{(\mu)} A_p^{(\sigma)} + \chi_{l2}^{\mu\sigma} A_a^{(\mu)} A_p^{(\sigma)*} \mathrm{e}^{i\Delta k^z z} \right\}, \tag{7}$$

$$\begin{aligned}&\frac{\partial A_s^{(\mu)}}{\partial z} + \frac{1}{v_s^{z(\mu)}} \frac{\partial A_s^{(\mu)}}{\partial t} \\ &= i \frac{2\pi\omega_s}{c n_s^{(\mu)} \cos\theta_s^z} \left\{ \chi_s^{\mu\sigma} A_l A_p^{(\sigma)*} + \gamma_{s1}^{\mu\mu'} \left|A_l\right|^2 A_s^{(\mu')} + \gamma_{s2}^{\mu\mu'\mu''} A_a^{(\mu)} A_a^{(\mu'')*} A_s^{(\mu'')} \right\}, \; \sigma = 1,2\end{aligned} \tag{8}$$

$$\begin{aligned}&2iW^z \frac{\partial A_p^{(\sigma)*}}{\partial z} - iW e_p^{(\sigma)z} \frac{\partial A_p^{(3)*}}{\partial z} + i \frac{2\omega_p \varepsilon_p^{(\sigma)*}}{c^2} \frac{\partial A_p^{(\sigma)*}}{\partial t} + \left(W^2 - k_p^{2*}\right) A_p^{(\sigma)*} \\ &= 4\pi q_p^2 \left\{ \chi_{p1}^{\mu\sigma} A_l^* A_s^{(\mu)} + \chi_{p2}^{\mu\sigma} A_l A_a^{(\mu)*} \mathrm{e}^{-i\Delta k^z z} \right\}\end{aligned} \tag{9}$$

$$\begin{aligned}&-iW\left(e_p^{(1)z} \frac{\partial A_p^{(1)*}}{\partial z} + e_p^{(2)z} \frac{\partial A_p^{(2)*}}{\partial z} \right) + i \frac{\mathrm{d}A_p^{(3)*}}{\mathrm{d}z} \left(W^z - W e_p^{(3)z}\right) + i \frac{2\omega_p \varepsilon_p^{(3)*}}{c^2} \frac{\partial A_p^{(3)*}}{\partial t} \\ &-k_p^{2*} A_p^{(3)*} = 4\pi q_p^2 \left\{ \chi_{p1}^{\mu3} A_l^* A_s^{(\mu)} + \chi_{p2}^{\mu3} A_l A_a^{(\mu)*} \mathrm{e}^{-i\Delta k^z z} \right\}\end{aligned} \tag{10}$$

Provided the strong polariton absorption we have [54]

$$\left| W \left(A_p^{(\sigma)} \right)^{-1} \frac{\partial A_p^{(\sigma)}}{\partial z} \right| \approx \left| \frac{\omega_p}{c^2} \left(A_p^{(\sigma)} \right)^{-1} \frac{\partial A_p^{(\sigma)}}{\partial t} \right| \ll \left| W^2 - k_p^{2*} \right|, \tag{11}$$

We can neglect in (9) and (10) the terms with the derivatives so that we could directly obtain the expressions for $A_p^{(\sigma)} (\sigma = 1,2)$ and $A_p^{(3)}$:

$$A_p^{(\sigma)*} = \frac{4\pi}{s^2 - \varepsilon_p^*} \left\{ \chi_{p1}^{\mu\sigma} A_l^* A_s^{(\mu)} + \chi_{p2}^{\mu\sigma} A_l A_a^{(\mu)*} \mathrm{e}^{-i\Delta k^z z} \right\}, (\sigma = 1,2), \tag{12}$$

and

$$A_p^{(3)*} = -\frac{4\pi}{\varepsilon_p^*} \left\{ \chi_{p1}^{\mu3} A_l^* A_s^{(\mu)} + \chi_{p2}^{\mu3} A_l A_a^{(\mu)*} \mathrm{e}^{-i\Delta k^z z} \right\}, \tag{13}$$

where $s = W/q_p$.

The substitution of the obtained expressions (12) and (13) for the amplitudes of polariton waves in (6)-(10) results in new system of differential equations for $A_{a,l,s}$ as follows:

$$\frac{\partial A_a^{(\mu)}}{\partial z}+\frac{1}{v_a^{z(\mu)}}\frac{\partial A_a^{(\mu)}}{\partial t}=i\frac{2\pi\omega_a}{cn_a^{(\mu)}\cos\theta_a^{z(\mu)}}\Big\{\overline{\gamma}_{a1}^{\mu\mu'\sigma}A_l^2A_s^{(\mu')*}\mathrm{e}^{-i\Delta k^z z}+\overline{\gamma}_{a2}^{\mu\mu'\sigma}\left|A_l\right|^2A_a^{(\mu')} + \gamma_{a2}^{\mu\mu'\mu''}A_s^{(\mu)}A_s^{(\mu')*}A_a^{(\mu'')}\Big\} \tag{14}$$

$$\frac{\partial A_l}{\partial z}+\frac{1}{v_l^{z}}\frac{\partial A_l}{\partial t}=i\frac{2\pi\omega_l}{cn_l\cos\theta_l^{z}}\Big\{\overline{\gamma}_{l11}^{\mu\mu'\sigma}A_lA_s^{(\mu)}A_s^{(\mu')*}+\overline{\gamma}_{l12}^{\mu\mu'\sigma}A_l^*A_s^{(\mu)}A_a^{(\mu')}\mathrm{e}^{i\Delta k^z z} + \overline{\gamma}_{l21}^{\mu\mu'\sigma}A_l^*A_s^{(\mu')}A_a^{(\mu)}\mathrm{e}^{i\Delta k^z z}+\overline{\gamma}_{l22}^{\mu\mu'\sigma}A_lA_a^{(\mu)}A_a^{(\mu')*}\Big\} \tag{15}$$

$$\frac{\partial A_s^{(\mu)}}{\partial z}+\frac{1}{v_s^{z(\mu)}}\frac{\partial A_s^{(\mu)}}{\partial t}=i\frac{2\pi\omega_s}{cn_s^{(\mu)}\cos\theta_s^{z}}\Big\{\overline{\gamma}_{s1}^{\mu\mu'\sigma}\left|A_l\right|^2A_s^{(\mu')}+\overline{\gamma}_{s2}^{\mu\mu'\sigma}A_l^2A_a^{(\mu')*}\mathrm{e}^{-i\Delta k^z z} + \gamma_{s2}^{\mu\mu'\mu''}A_a^{(\mu')}A_a^{(\mu'')*}A_s^{(\mu''')}\Big\} \tag{16}$$

where

$$\overline{\gamma}_{a1}^{\mu\mu'\sigma}\equiv 4\pi\left(\frac{\chi_a^{\mu\sigma}\chi_{p1}^{\mu'\sigma}}{s^2-\varepsilon_p}-\frac{\chi_a^{\mu3}\chi_{p1}^{\mu'3}}{\varepsilon_p}\right),\quad \overline{\gamma}_{a2}^{\mu\mu'\sigma}\equiv 4\pi\left(\frac{\chi_a^{\mu\sigma}\chi_{p1}^{\mu'\sigma}}{s^2-\varepsilon_p}-\frac{\chi_a^{\mu3}\chi_{p2}^{\mu'3}}{\varepsilon_p}\right)+\gamma_{a2}^{\mu\mu'},$$

$$\overline{\gamma}_{l11}^{\mu\mu'\sigma}\equiv 4\pi\chi_{l1}^{\mu\sigma}\left(\frac{\chi_{p1}^{\mu'\sigma}}{s^2-\varepsilon_p}-\frac{\chi_{p1}^{\mu'3}}{\varepsilon_p}\right),\quad \overline{\gamma}_{l12}^{\mu\mu'\sigma}\equiv 4\pi\chi_{l1}^{\mu\sigma}\left(\frac{\chi_{p2}^{\mu'\sigma}}{s^2-\varepsilon_p}-\frac{\chi_{p2}^{\mu'3}}{\varepsilon_p}\right),$$

$$\overline{\gamma}_{l21}^{\mu\mu'\sigma}\equiv 4\pi\chi_{l2}^{\mu\sigma}\left(\frac{\chi_{p1}^{\mu'\sigma}}{s^2-\varepsilon_p^*}-\frac{\chi_{p1}^{\mu'3}}{\varepsilon_p^*}\right),\quad \overline{\gamma}_{l22}^{\mu\mu'\sigma}\equiv 4\pi\chi_{l2}^{\mu\sigma}\left(\frac{\chi_{p2}^{\mu'\sigma}}{s^2-\varepsilon_p^*}-\frac{\chi_{p2}^{\mu'3}}{\varepsilon_p^*}\right)$$

$$\overline{\gamma}_{s1}^{\mu\mu'\sigma}\equiv \gamma_{s1}^{\mu\mu'}+4\pi\chi_{s}^{\mu\sigma}\left(\frac{\chi_{p1}^{\mu'\sigma}}{s^2-\varepsilon_p^*}-\frac{\chi_{p1}^{\mu'3}}{\varepsilon_p^*}\right),\quad \overline{\gamma}_{s2}^{\mu\mu'\sigma}\equiv 4\pi\chi_{s}^{\mu\sigma}\left(\frac{\chi_{p2}^{\mu'\sigma}}{s^2-\varepsilon_p^*}-\frac{\chi_{p2}^{\mu'3}}{\varepsilon_p^*}\right).$$

The system (14)-(16) can also be simplified if we introduce new variables as

$$A_a^{'(\mu)}\equiv A_a^{(\mu)}\mathrm{e}^{i\Delta k^z z/2},\quad A_s^{'(\mu)}\equiv A_s^{(\mu)}\mathrm{e}^{i\Delta k^z z/2} \tag{17}$$

Assuming the "week" wave mismatch between waves at Stokes and anti-Stokes frequencies, that is

$$\left|\frac{\partial A_{a,s}^{'(\mu)}}{\partial z}+\frac{1}{v_{a,s}^{z(\mu)}}\frac{\partial A_{a,s}^{'(\mu)}}{\partial t}\right|\gg\frac{\Delta k^z}{2}A_{a,s}^{'(\mu)}, \tag{18}$$

and after bringing all variables to the unitless form, the system of nonstationary equations simulating CARS can be rewritten as follows:

$$\frac{\partial\tilde{A}_a^{'(\mu)}}{\partial\tilde{z}}+\frac{1}{\tilde{v}_a^{z(\mu)}}\frac{\partial\tilde{A}_a^{'(\mu)}}{\partial\tilde{t}} = i\Big\{C_{a1}^{\mu\mu'}\tilde{A}_l^2\tilde{A}_s^{'(\mu')*}+C_{a2}^{\mu\mu'}\left|\tilde{A}_l\right|^2\tilde{A}_a^{'(\mu')}+C_{a2}^{\mu\mu'\mu''}\tilde{A}_s^{'(\mu)}\tilde{A}_s^{'(\mu')*}\tilde{A}_a^{'(\mu'')}\Big\} \tag{19}$$

$$\frac{\partial\tilde{A}_l}{\partial\tilde{z}}+\frac{1}{\tilde{v}_l^{z}}\frac{\partial\tilde{A}_l}{\partial\tilde{t}}=i\Big\{C_{l11}^{\mu\mu'}\tilde{A}_l\tilde{A}_s^{'(\mu)}\tilde{A}_s^{'(\mu')*}+C_{l12}^{\mu\mu'}\tilde{A}_l^*\tilde{A}_s^{'(\mu)}\tilde{A}_a^{'(\mu')} + C_{l21}^{\mu\mu'}\tilde{A}_l^*\tilde{A}_s^{'(\mu')}\tilde{A}_a^{'(\mu)}+C_{l22}^{\mu\mu'}\tilde{A}_l\tilde{A}_a^{'(\mu)}\tilde{A}_a^{'(\mu')*}\Big\} \tag{20}$$

$$\frac{\partial \tilde{A}_s^{'(\mu)}}{\partial \tilde{z}} + \frac{1}{\tilde{v}_s^{z(\mu)}} \frac{\partial \tilde{A}_s^{'(\mu)}}{\partial \tilde{t}} = i\left\{ C_{s1}^{\mu\mu'} \left|\tilde{A}_l\right|^2 \tilde{A}_s^{'(\mu')} + C_{s2}^{\mu\mu'} \tilde{A}_l^2 \tilde{A}_a^{'(\mu')*} + C_{s2}^{\mu\mu'\mu''} \tilde{A}_a^{'(\mu)} \tilde{A}_a^{'(\mu')*} \tilde{A}_s^{'(\mu'')} \right\} \tag{21}$$

where $\tilde{A}_{a,s}^{'(\mu)} \equiv A_{a,s}^{'(\mu)} / A_0$, $\tilde{A}_l \equiv A_l / A_0$, $\tilde{t} \equiv t/\tau_0$ (A_0 and τ_0 are the peak amplitude and characteristic pulse duration of the pump, $z_0 = c\tau_0$, c is the speed of light in vacuum),

$$\begin{gathered}
C_{a1}^{\mu\mu'} \equiv \frac{2\pi\omega_a z_0}{cn_a^{(\mu)} \cos\theta_a^{z(\mu)}} \overline{\gamma}_{a1}^{\mu\mu'\sigma} A_0^2; \quad C_{a2}^{\mu\mu'} \equiv \frac{2\pi\omega_a z_0}{cn_a^{(\mu)} \cos\theta_a^{z(\mu)}} \overline{\gamma}_{a2}^{\mu\mu'\sigma} A_0^2; \\
C_{a2}^{\mu\mu'\mu''} \equiv \frac{2\pi\omega_a z_0}{cn_a^{(\mu)} \cos\theta_a^{z(\mu)}} \overline{\gamma}_{a2}^{\mu\mu'\mu''} A_0^2; \quad C_{l11}^{\mu\mu'} \equiv \frac{2\pi\omega_l z_0}{cn_l \cos\theta_l^{z}} \overline{\gamma}_{l11}^{\mu\mu'\sigma} A_0^2; \\
C_{l12}^{\mu\mu'} \equiv \frac{2\pi\omega_l z_0}{cn_l \cos\theta_l^{z}} \overline{\gamma}_{l12}^{\mu\mu'\sigma} A_0^2; \quad C_{l21}^{\mu\mu'} \equiv \frac{2\pi\omega_l z_0}{cn_l \cos\theta_l^{z}} \overline{\gamma}_{l21}^{\mu\mu'\sigma} A_0^2; \\
C_{l22}^{\mu\mu'} \equiv \frac{2\pi\omega_l z_0}{cn_l \cos\theta_l^{z}} \overline{\gamma}_{l22}^{\mu\mu'\sigma} A_0^2; \quad C_{s1}^{\mu\mu'} \equiv \frac{2\pi\omega_s z_0}{cn_s^{(\mu)} \cos\theta_s^{z}} \overline{\gamma}_{s1}^{\mu\mu'\sigma} A_0^2; \\
C_{s2}^{\mu\mu'} \equiv \frac{2\pi\omega_s z_0}{cn_s^{(\mu)} \cos\theta_s^{z}} \overline{\gamma}_{s2}^{\mu\mu'\sigma} A_0^2; \quad C_{s2}^{\mu\mu'\mu''} \equiv \frac{2\pi\omega_s z_0}{cn_s^{(\mu)} \cos\theta_s^{z}} \overline{\gamma}_{s2}^{\mu\mu'\mu''} A_0^2;
\end{gathered} \tag{22}$$

3. Asymptotic Solutions in a Form of Simultons at Frequencies $\omega_{a,l,s}$

Here, we are looking for stationary solutions for the system mentioned above as (the tensors C in (22) are supposed to be previously diagonalized)

$$\tilde{A}_{a,s}^{'(\mu)}\left(\tilde{z},\tilde{t}\right) \equiv B_{a,s}^{(\mu)}\left(\tilde{\xi}\right) \mathrm{e}^{i\Phi_{a,s}^{(\mu)}(\tilde{\xi})}, \quad \tilde{A}_l\left(\tilde{z},\tilde{t}\right) \equiv B_l\left(\tilde{\xi}\right) \mathrm{e}^{i\Phi_l(\tilde{\xi})}, \tag{23}$$

where $\tilde{\xi} \equiv \tilde{t} - \tilde{z}/\tilde{v}^z$; $\tilde{v}^z$ is the velocity of simultons at the frequencies $\omega_{a,l,s}$; $B_{a,l,s}^{(\mu)}$ and $\Phi_{a,l,s}^{(\mu)}$ are the real amplitudes and phases of the interacting waves, respectively. Since we are going to evaluate amplitudes and phases separately, we duplicate the system (19)-(21) by using a standard procedure of presenting the real and imaginary parts of those equations as different ones:

$$\frac{\mathrm{d}B_a^{(\mu)}}{\mathrm{d}\tilde{\xi}} = -\kappa_a^{(\mu)} C_{a1}^{\mu\mu} B_l^2 B_s^{(\mu)} \sin\Phi, \tag{24}$$

$$\frac{\mathrm{d}\Phi_a^{(\mu)}}{\mathrm{d}\tilde{\xi}} = \kappa_a^{(\mu)} C_{a1}^{\mu\mu} \frac{B_l^2 B_s^{(\mu)}}{B_a^{(\mu)}} \cos\Phi + \kappa_a^{(\mu)} \left(C_{a2}^{\mu\mu} B_l^2 + C_a^{\mu\mu\mu} B_s^{(\mu)2} \right) \tag{25}$$

$$\frac{\mathrm{d}B_l}{\mathrm{d}\tilde{\xi}} = \kappa_l \left(C_{l12}^{\mu\mu} + C_{l21}^{\mu\mu} \right) B_l B_s^{(\mu)} B_a^{(\mu)} \sin\Phi \tag{26}$$

$$\frac{\mathrm{d}\Phi_l}{\mathrm{d}\tilde{\xi}} = \kappa_l \left(C_{l12}^{\mu\mu} + C_{l21}^{\mu\mu} \right) B_s^{(\mu)} B_a^{(\mu)} \cos\Phi + \kappa_l C_{l11}^{\mu\mu} B_s^{(\mu)2} + \kappa_l C_{l22}^{\mu\mu} B_a^{(\mu)2} \tag{27}$$

$$\frac{\mathrm{d}B_s^{(\mu)}}{\mathrm{d}\tilde{\xi}} = -\kappa_s^{(\mu)} C_{s2}^{\mu\mu} B_l^2 B_a^{(\mu)} \sin\Phi, \tag{28}$$

$$\frac{\mathrm{d}\Phi_s^{(\mu)}}{\mathrm{d}\tilde{\xi}} = \kappa_s^{(\mu)} \left\{ C_{s1}^{\mu\mu} B_l^2 + C_{s2}^{\mu\mu\mu} B_a^{(\mu)2} + C_{s2}^{\mu\mu} \frac{B_l^2 B_a^{(\mu)}}{B_s^{(\mu)}} \cos\Phi \right\} \tag{29}$$

where

$$\kappa_{a,s}^{(\mu)} \equiv \tilde{v}_{a,s}^{z(\mu)} \tilde{v}^z \Big/ \left(\tilde{v}^z - \tilde{v}_{a,s}^{z(\mu)}\right), \quad \kappa_l \equiv \tilde{v}_l^z \tilde{v}^z \Big/ \left(\tilde{v}^z - \tilde{v}_l^z\right), \tag{30}$$

$$\Phi \equiv 2\Phi_l - \Phi_s^{(\mu)} - \Phi_a^{(\mu)}.$$

Then if we introduce the amplitude of simultons as

$$Q \equiv \frac{B_a^{(\mu)2}}{\lambda_a^{(\mu)2}} = \frac{B_l^2}{\lambda_l^2} = \frac{B_s^{(\mu)2}}{\lambda_s^{(\mu)2}}, \tag{31}$$

we can reduce the above system to

$$\frac{\mathrm{d}Q}{\mathrm{d}\tilde{\xi}} = \alpha Q^2 \sin\Phi, \tag{32}$$

$$\frac{\mathrm{d}\Phi}{\mathrm{d}\tilde{\xi}} = 2\alpha Q \cos\Phi + \beta Q, \tag{33}$$

Where

$$\lambda_a^{(\mu)2} \equiv -\kappa_a^{(\mu)} C_{a1}^{\mu\mu}, \quad \lambda_l^2 \equiv \kappa_l \left(C_{l12}^{\mu\mu} + C_{l21}^{\mu\mu}\right), \tag{34}$$

$$\lambda_s^{(\mu)2} \equiv -\kappa_s^{(\mu)} C_{s2}^{\mu\mu}, \quad \alpha \equiv 2\lambda_a^{(\mu)} \lambda_l^2 \lambda_s^{(\mu)},$$

$$\beta \equiv \left(2\kappa_l C_{l22}^{\mu\mu} - \kappa_s^{(\mu)} C_{s2}^{\mu\mu\mu}\right) \lambda_a^{(\mu)2} - \left(\kappa_s^{(\mu)} C_{s1}^{\mu\mu} + \kappa_a^{(\mu)} C_{a2}^{\mu\mu}\right) \lambda_l^2$$

$$+ \left(2\kappa_l C_{l11}^{\mu\mu} - \kappa_a^{(\mu)} C_a^{\mu\mu\mu}\right) \lambda_s^{(\mu)2}.$$

The system (32)-(33) can be rewritten as,

$$\frac{\mathrm{d}Q}{\mathrm{d}x} = Q^2 \sin\Phi, \tag{35}$$

$$\frac{\mathrm{d}\Phi}{\mathrm{d}x} = Q\left(\tilde{\beta} + 2\cos\Phi\right), \tag{36}$$

where $x = \alpha\tilde{\xi}$, $\tilde{\beta} = \beta/\alpha$. The numerical solutions of that system as polarized sumultons are shown in **Figure 1**.

The transient processes of simultons formation for pulses at the pump, Stokes, and anti-Stokes frequencies are shown in **Figure 2**.

4. Gain Factor g_μ

It can also be shown that the system of Equations (10)-(21) is consistent with the experimental results for CARS by polaritons. To facilitate the analysis we consider the stationary solutions for Stokes and anti-Stokes waves in the constant pump approximation. Here we also assume that the processes of SRS ω_l and the mutual interaction between ω_s and ω_a dominate other processes. Under that assumption the equations (19) and (21) can be reduced to the following

$$\frac{\mathrm{d}\tilde{A}_a^{1(\mu)*}}{\mathrm{d}z} = \kappa_a^* \tilde{A}_s^{1(\mu)} \tag{37}$$

$$\frac{d\tilde{A}_s^{1(\mu)}}{dz} = \kappa_s \tilde{A}_a^{1(\mu)*} \tag{38}$$

where $\kappa_a^{\nu} = -iC_{a1}^{\mu\mu}$; $\kappa_s = iC_{s2}^{\mu\mu}$. We have also assumed that tensors were diagonalized.

This system can be converted into the single equation of the second order for, for example, the wave at Stokes frequency:

$$\frac{d^2\tilde{A}_s^{1(\mu)}}{dz^2} = \kappa_s \kappa_a^* \tilde{A}_s^{1(\mu)} \tag{39}$$

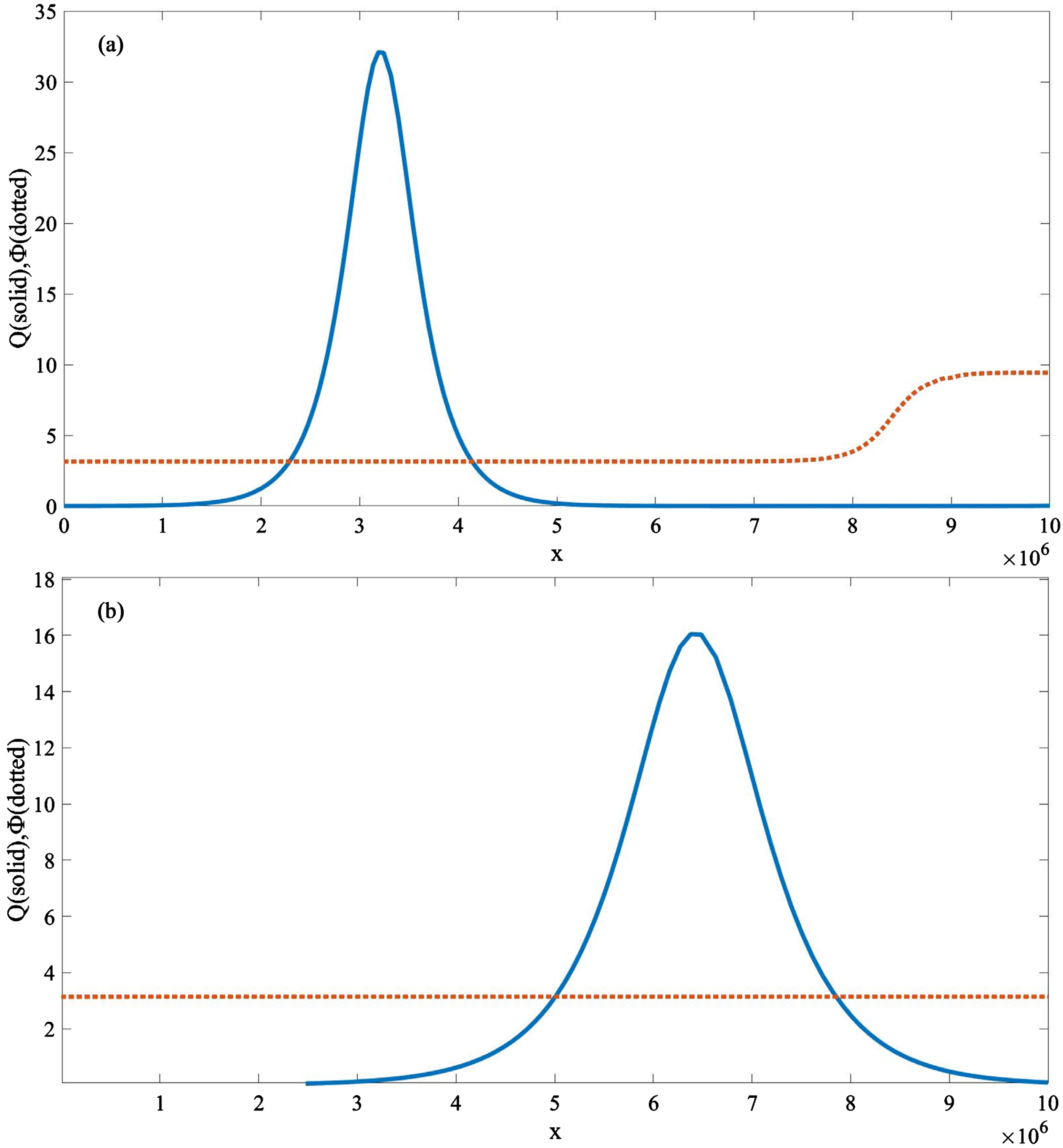

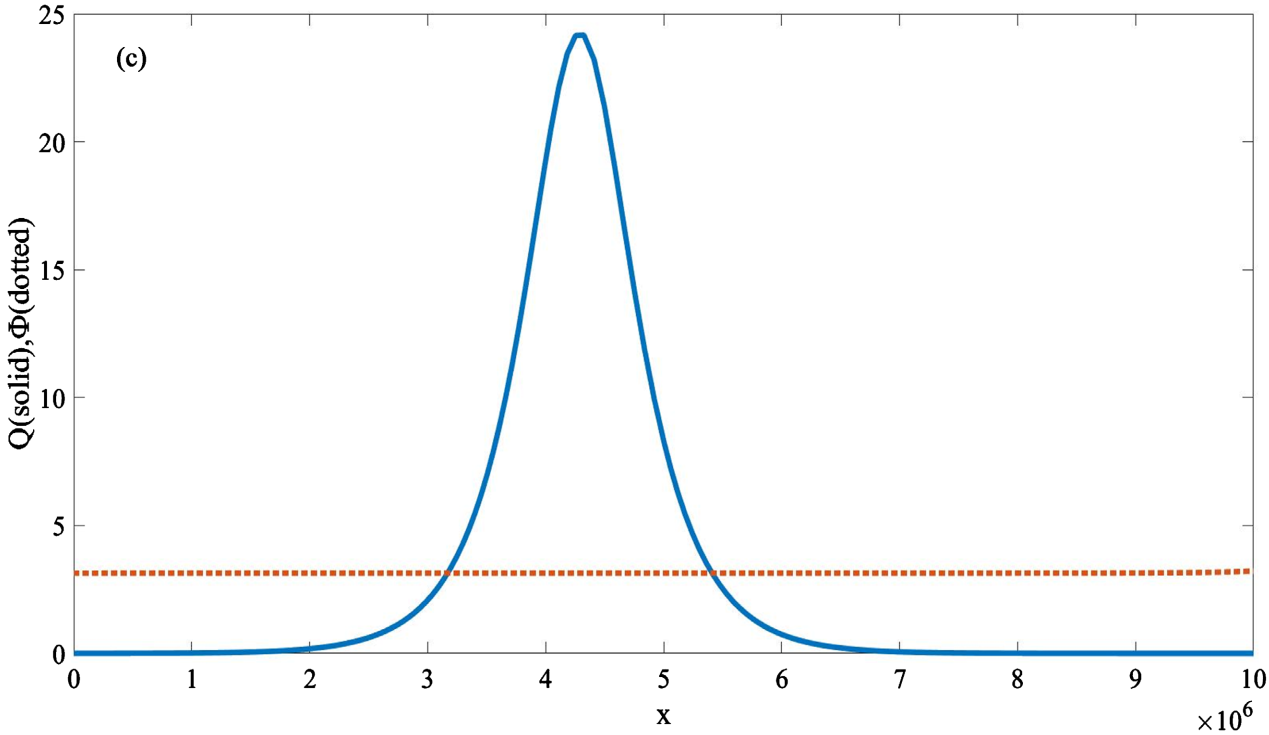

Figure 1. The numerical solutions of (35)-(36) for polarized sumultons different initial conditions: (a) $Q(0) = 0.002$, $\Phi = \pi$; (b) $Q(0) = 0.001$, $\Phi = \pi$; (c) $Q(0) = 0.0015$,, $\Phi = \pi$.

Finally, if we introduce the gain factor as

$$\tilde{A}_s^{1(\mu)}(z) = \tilde{A}_s^{(\mu)}(0)\mathrm{e}^{gz}, \tag{40}$$

Then we would obtain g after substituting (40) in (39):

$$\begin{aligned} g &\approx \left(\kappa_a^*\kappa_s\right)^{\frac{1}{2}} = \left(C_{a1}^{\mu\mu}C_{s2}^{\mu\mu}\right)^{\frac{1}{2}} \\ &= \left(\frac{2\pi\omega_a z_a}{cn_a^{(\mu)}\cos\theta_a^{z(\mu)}}\tilde{\gamma}_{a1}^{\mu\mu\sigma}A_0^2\frac{2\pi\omega_s z_0}{cn_s^{(\mu)}\cos\theta_s^{z(\mu)}}\tilde{\gamma}_{s2}^{\mu\mu\sigma}A_0^2\right)^{\frac{1}{2}} \\ &\approx 8\pi^2\omega z_0\chi^2A_0^2/(cn); \end{aligned} \tag{41}$$

(here we assumed that the pump was strong enough to provide $C_{a1}C_{s1} \gg \left(\frac{\Delta k^z}{2}\right)^2$).

As the experimental data for this gain, we used the following [56]: pulse width of the pulsed Ar^+ laser $\simeq$ 30 ps, the peak output power ≈ 2.5 kW, the wavelength was 514.5 nm, the cross-section ≈ 10^{-18} cm^{-2}, $\gamma_f \approx 10\ \mathrm{cm}^{-1}$, and $\chi \approx 10^{-8}$ esu. In [57] the nonlinear medium was zinc blende ZnS, in which the polariton frequencies were in the rage 200 - 400 cm^{-1}. Both the experimental results for the gain factor in [55] and calculations based on (41) have resulted in g ≈ 1 and are shown in **Figure 3**.

5. Conclusion

In this paper, we theoretically showed that in the case of transient SRS by polaritons,

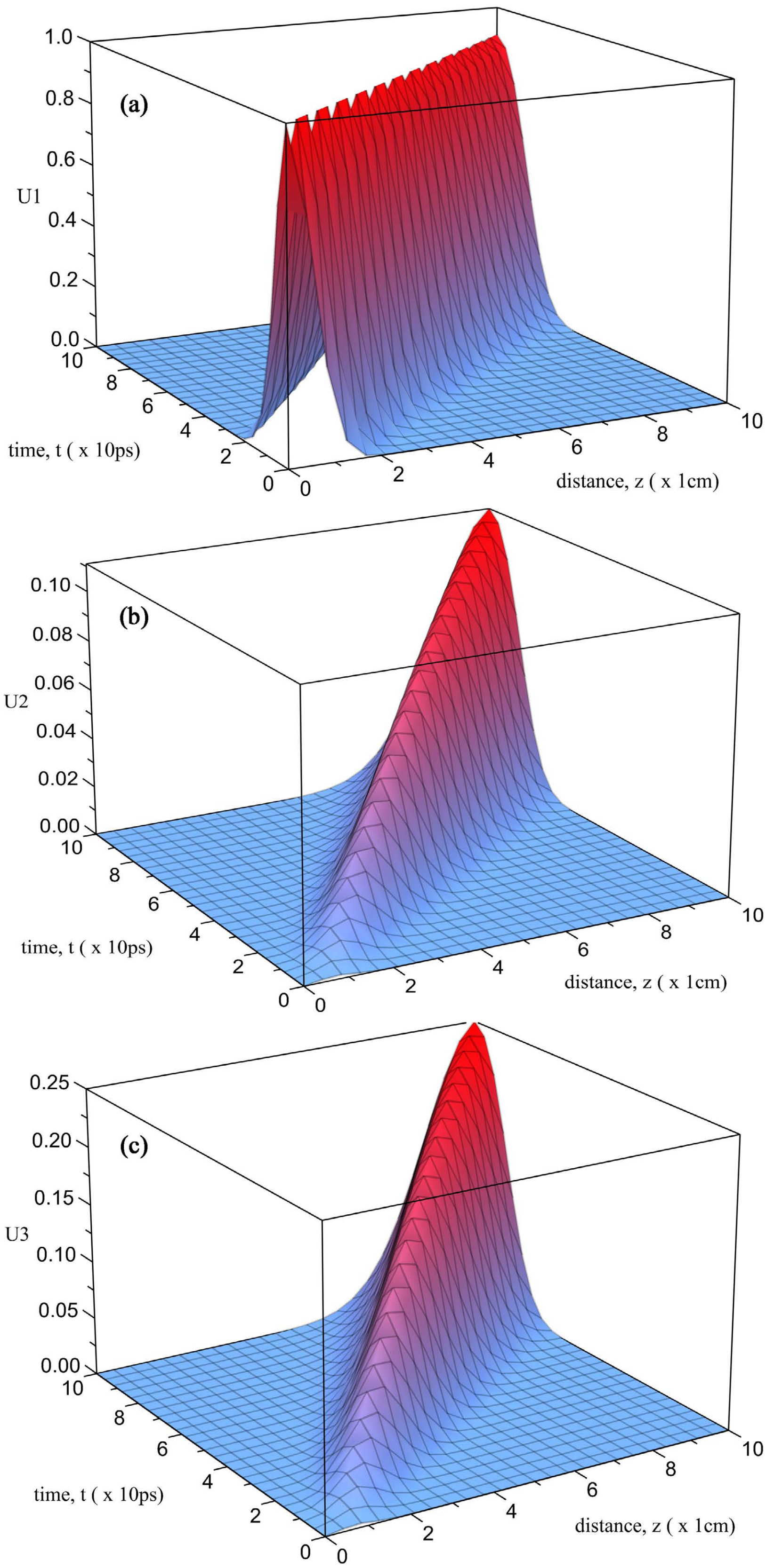

Figure 2. The computer simulation of transient processes for unitless intensities for (a) pump; (b) Stokes, and (c) anti-Stokes.

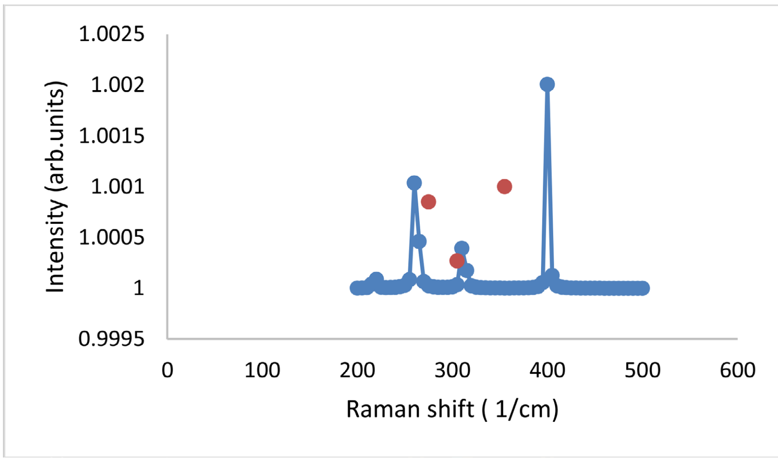

Figure 3. Gain factor versus polariton frequency in zinc blende ZnS. The red dots correspond to the experimental points ([57]); blue solid lines are the result of a calculation based on ([41]).

there is a possibility of occurrence of simultaneously propagating ultrafast stable pulses (simultons) not only at different frequencies but with different polarizations as well. It was found that those polarizations are mutually perpendicular and perpendicular to the direction of propagation. Such features can be used in optoelectronics in polarization filters and as an analog of bits in digital optical communication systems.

Conflicts of Interest

The authors declare no conflicts of interest regarding the publication of this paper.

References

[1] Driben, R., Kartashov, Y.V., Malomed, B.A., Meier, T. and Tovner, L. (2014) Three-Dimensional Hybrid Vortex Solitons. *New Journal of Physics*, **16**, 2-16. https://doi.org/10.1088/1367-2630/16/6/063035

[2] Smirnov, L.A., Smirnova, D.A., Ostrovskaya, E.A. and Kivshar, Y.S. (2014) Dynamics and Stability of Dark Solitons in Exciton-Polariton Condensates. *Physical Review B*, **89**, Article ID: 235310. https://doi.org/10.1103/PhysRevB.89.235310

[3] Dzedolik, I.V. and Minov, I. (2016) Solitons and Nonlinear Waves of Phonon-Polaritons and Plasmol-Polaritons. Nova Science Pub Inc., Hauppauge, 151 p.

[4] Yoshimura, M. and Sasao, N. (2014) Two-Photon Paired Solitons Supported by Medium Polarization. *Progress of Theoretical and Experimental Physics*, **2014**, 073B02. https://doi.org/10.1093/ptep/ptu094

[5] Kalashnikov, V.L. and Sorokin, E. (2014) Dissipative Raman Solitons. *Optics Express*, **22**, 30118-30126. https://doi.org/10.1364/OE.22.030118

[6] Uzunov, I.M. and Arabadzhiev, T.N. (2019) Intrapulse Raman Scattering and Dissipative Solitons with Extreme Spikes. *Applied Physics B*, **125**, 221. https://doi.org/10.1007/s00340-019-7332-7

[7] Xu, Y., Suarez, P., Milovic, D, Khan, K.R., Mahmood, M.F. and Diswas, A. (2016) Raman Solitons in Nanoscale Optical Waveguides, with Metamaterials, Having Po-

lynomial Law Non-Linearity. *Journal of Modern Optics*, **63**, 532-537. https://doi.org/10.1080/09500340.2016.1193240

[8] Boiti, M., Caputo, J.-G., Leon, J. and Pempinelli, F. (2000) Raman Solitons in Transient SRS. *Inverse Problems*, **16**, 303. https://doi.org/10.1088/0266-5611/16/2/303

[9] Wilson, K.S.J. and Navaneethakrishnan (2011) Effect of Nonlinear Interactions on Phonon Polariton Modes in Optoelectronic Crystals. *International Journal of Modern Physics B*, **25**, 1681-1688. https://doi.org/10.1142/S021797921105895X

[10] Xu, P., Zhu, S.N., Yu, X.Q., Ji, S.H., Gao, Z.D., Zhao, G., Zhu, Y.Y. and Ming, N.B. (2005) Experimental Studies of Enhanced Raman Scattering from a Hexagonally Poled $LiTaO_3$ Crystal. *Physical Review B*, **72**, Article ID: 064307. https://doi.org/10.1103/PhysRevB.72.064307

[11] Ema, K. and Kuwata-Gonokami, M. (1995) Soliton like Propagation of Exciton-Polariton Pulses Supported by Biexciton Two-Photon Dispersion. *Physical Review Letters*, **75**, 224. https://doi.org/10.1103/PhysRevLett.75.224

[12] Stoychev, K.T. and Primatarowa, M.T. (1992) Spatial Dispersion Effects in Polariton Solitons. *Physical Review B*, **46**, 10727. https://doi.org/10.1103/PhysRevB.46.10727

[13] Baumgartner, M.O., Scherrer, D.P. and Kneubuhl, F.K. (1998) Stimulated Raman Scattering and Spontaneous Raman Solitons in Ammonia. *Infrared Physics and Technology*, **39**, 457-472. https://doi.org/10.1016/S1350-4495(98)00029-2

[14] Di Paola, D.M., Walker, P.M., Emmanuele, R.P.A., Yulin, A.V., *et al*. (2021) Ultrafast-Nonlinear Ultraviolet Pulse Modulation in an AlInGaN Polariton Waveguide Operating Up to Room Temperature. *Nature Communications*, **12**, 3504. https://doi.org/10.1038/s41467-021-23635-6

[15] Liu, Q., Li, N. and Tan, C. (2020) All-Optical Logic Gate Based on Manipulation of Surface Polariton Solitons via External Gradient Magnetic Fields. *Physical Review A*, **101**, Article ID: 023818. https://doi.org/10.1103/PhysRevA.101.023818

[16] Rowe, W.R., Skryabin, D.V. and Gorbach, A.V. (2020) Raman Solitons in Waveguides with Simultaneous Quadratic and Kerr Nonlinearities. *Physical Review A*, 102, Article ID: 023523. https://doi.org/10.1103/PhysRevA.102.023523

[17] Yu, M., Okawachi, Y., Cheng, R., *et al*. (2020) Raman Lasing and Soliton Mode-Locking in Lithium Niobate Microresonators. *Light*: *Science and Applications*, **9**, Article No. 9. https://doi.org/10.1038/s41377-020-0246-7

[18] Milario, L.M.L., Bruchhausen, A., Lobos, A.M. and Aligia, A.A. (2007) Theory of Polariton-Mediated Raman Scattering in Microcavities. *Journal of Physics*: *Condensed Matter*, **19**, Article ID: 176210. https://doi.org/10.1088/0953-8984/19/17/176210

[19] Sich, M., Krizhanovskii, D.N., *et al*. (2012) Observation of Bright Polariton Solitons in a Semiconductor Microcavity. *Nature Photonics*, **6**, 50-55. https://doi.org/10.1038/nphoton.2011.267

[20] Sich, M., Tapia-Rodriguez, L.E., Sigurdsson, H., *et al*. (2018) Spin Domains in One-Dimensional Conservative Polariton Solitons. *ACS Photonics*, **5**, 5095-5102. https://doi.org/10.1021/acsphotonics.8b01410

[21] Sich, M., Skryabin, D.V. and Krizhanovskii (2016) Soliton Physics with Semiconductor Exciton-Polaritons in Confined Systems. *Comptes Rendus Physique*, **17**, 908-919. https://doi.org/10.1016/j.crhy.2016.05.002

[22] Volkel, A., Nimmesgern, L., Mielnik-Pyszczorski, A., Wirth, T. and Herink, G. (2022) Intracavity Raman Scattering Couples Soliton Molecules with Terahertz Phonons. *Nature Communications*, **13**, 2066.

https://doi.org/10.1038/s41467-022-29649-y

[23] Anashkina, E.A., Marisova, M.P. and Andrianov, A.V. (2022) Thermo-Optical Control of Raman Solitons in a Functionalized Silica Microsphere. *Micromachines*, **13**, 1616. https://doi.org/10.3390/mi13101616

[24] Viscarra, M.A. and Urzagasti, D. (2022) Dark Soliton Solutions of the Cubic-Quintic Complex Ginzburg-Landau Equation with High-Order Terms and Potential Barriers in Normal-Dispersion Fiber Lasers. *Journal of Nonlinear Optical Physics & Materials*, **31**, Article ID: 2250003. https://doi.org/10.1142/S0218863522500035

[25] Ma, P., Lin, W., Zhang, H., Xu, S. and Yang, Z. (2019) High-Power Large-Energy Raman Soliton Generations within a Mode-Locked Yb-Doped Fiber Laser Based on High-Damage-Threshold CVD-MoS2 as Modulator. *Nanomaterials*, **9**, 1305. https://doi.org/10.3390/nano9091305

[26] Li, Z., Li, N., Yao, C., *et al.* (2018) Tunable Mid-Infrared Raman Soliton Generation from 1.96 to 2.82 μm in an All-Solid Fluoro-Tellurite Fiber. *AIP Advances*, **8**, Article ID: 115001. https://doi.org/10.1063/1.5042137

[27] Rodriguez, P., Jesus, J., Guillet, T. and Ackermann, T. (2017) Polarization Properties of Laser Solitons. *Applied Sciences*, **7**, 442. https://doi.org/10.3390/app7050442

[28] Fu, Y., Zhang W.L. and Wu, X.M. (2015) Polarization-Dependent Solitons in the Strong Coupling Regime of Semiconductor Microcavities. *Chaos*, *Solitons & Fractals*, **81**, 345-350. https://doi.org/10.1016/j.chaos.2015.10.015

[29] Rosas, A.F., Hernández, O.D., Arceo, R., *et al.* (2018) Polarization Properties of the Solitons Generated in the Process of Pulse Breakup in Twisted Fiber Pumped by ns Pulses. In: Lembrikov, B.I., Ed., *Nonlinear Optics*, Intechopen, London, 73-88.

[30] Luan, F., Yulin, A.V., Knight, J.C. and Skryabin, D.V. (2006) Polarization Instability of Solitons in Photonic Crystal Fibers. *Optics Express*, **14**, 6550-6556. https://doi.org/10.1364/OE.14.006550

[31] Triki, H., Biswas, A., Moshokoa, S.P. and Belic, M. (2017) Optical Solitons and Conservation Laws with Quadratic-Cubic Nonlinearity. *Optik*, **128**, 63-70. https://doi.org/10.1016/j.ijleo.2016.10.010

[32] Li, B.-Q. and Ma, Y.L. (2017) Periodic Solutions and Solitons to Two Complex Short Pulse (CSP) Equations in Optical Fiber. *Optik*, **144**, 149-155. https://doi.org/10.1016/j.ijleo.2017.06.114

[33] Arshad, M.., Seadawy, A.R. and Lu, D. (2017) Exact Bright-Dark Solitary Wave Solutions of the Higher-Order Cubic-Quintic Nonlinear Schrödinger Equation and Its Stability. *Optik*, **138**, 40-49. https://doi.org/10.1016/j.ijleo.2017.03.005

[34] Kibler, B., Fatome, J., Finot, C., *et al.* (2010) The Peregrine Soliton in Nonlinear Fiber Optics. *Nature Physics*, **6**, 790-795. https://doi.org/10.1038/nphys1740

[35] Li, B.-Q., Sun. J.-Z. and Ma. Y.-L. (2018) Soliton Excitation for a Coherently Coupled Nonlinear Schrödinger System in Optical Fibers with Two Orthogonally Polarized Components. *Optik*, **175**, 275-283. https://doi.org/10.1016/j.ijleo.2018.08.108

[36] Li, B.-Q. and Ma, Y.-L. (2019) Periodic and *N*-Kink-Like Optical Solitons for a Generalized Schrödinger Equation with Variable Coefficients in an Inhomogeneous Fiber System. *Optik*, **179**, 854-860. https://doi.org/10.1016/j.ijleo.2018.11.008

[37] Yang, J.-W., Gao, Y.-T., Su, C.-Q., Zuo, D.-W. and Feng, Y.-J. (2017) Solitons and Quasi-Periodic Behaviors in an Inhomogeneous Optical Fiber. *Communications in Nonlinear Science and Numerical Simulation*, **42**, 477-490.

https://doi.org/10.1016/j.cnsns.2016.05.013

[38] Hoque, M.-F. and Roshid, H.-O. (2020) Optical Soliton Solutions of the Biswas-Arshed Model by the Expansion Method. *Physica Scripta*, **95**, Article ID: 075219. https://doi.org/10.1088/1402-4896/ab97ce

[39] Ullah, M.S., Roshid, H.O., Ali, M.Z. and Rahman, Z. (2019) Novel Exact Solitary Wave Solutions for the Time Fractional Generalized Hirota-Satsuma Coupled KdV Model through the Generalized Kudryshov Method. *Contemporary Mathematics*, **1**, 25-32. https://doi.org/10.37256/cm.11201936.25-33

[40] Ullah, M.S., Roshid, H.O., Ali, M.Z. and Rahman, Z. (2020) Dynamical Structures of Multi-Soliton Solutions to the Bogoyavlenskii's Breaking Soliton Equations. *The European Physical Journal Plus*, **135**, 282. https://doi.org/10.1140/epjp/s13360-020-00289-9

[41] Eslami, M., Hosseini, K., Matinfar, M., *et al.* (2021) A Nonlinear Schrödinger Equation Describing the Polarization Mode and Its Chirped Optical Solitons. *Optical and Quantum Electronics*, **53**, 314. https://doi.org/10.1007/s11082-021-02917-9

[42] Ferreira. M.F.S. (2008) Soliton Transmission in Fibers with Polarization-Mode Dispersion. *Fiber and Integrated Optics*, **27**, 113-126. https://doi.org/10.1080/01468030802040063

[43] Chen, W., Xu, W., Luo, A., *et al.* (2006) Enhanced Polarization Soliton's Robustness to Polarization Mode Dispersion in Fiber Systems with Frequency-Dependent Loss. *Modern Physics Letters B* **20**, 1023-1031. https://doi.org/10.1142/S0217984906011098

[44] Zhang, H., Tang, D.Y., Zhao, L.M. and Wu, X. (2009) Observation of Polarization Domain Wall Solitons in Weakly Birefringent Cavity Fiber Lasers. *Physical Review B*, **80**, Article ID: 052302. https://doi.org/10.1103/PhysRevB.80.052302

[45] Klein, A., Meir, S., Duadi, H., *et al.* (2021) Polarization Dynamics of Ultrafast Solitons. *Optics Express*, **29**, 18512-8522. https://doi.org/10.1364/OE.426122

[46] Zhao, L.M., Tang, D.Y., Wu, X., Zhang, H. and Tam, H.Y. (2009) Coexistence of Polarization-Locked and Polarization-Rotating Vector Solitons in a Fiber Laser with SESAM. *Optics Letters*, **34**, 3059-3061. https://doi.org/10.1364/OL.34.003059

[47] Ivanov, A.L., Haug, H. and Vygovskii, G.S. (1996) Coupled Solitons in Resonant Raman Interaction of Intense Polaritons. *Physical Review B*, **53**, 13482. https://doi.org/10.1103/PhysRevB.53.13482

[48] Marchevskii, F.N., Strizhevskii, V.L. and Feshchenko, V.P. (1984) Soliton Generation in Stimulated Raman Scattering and Excitation of Polar Optical Phonons. *Soviet Journal of Quantum Electronics*, **14**, 192. https://doi.org/10.1070/QE1984v014n02ABEH004691

[49] Feshchenko, V. and Feshchenko, G. (2020) Nonstationary CARS by Polaritons. *Journal of Applied Mathematics and Physics*, **8**, 1949-1958. https://doi.org/10.4236/jamp.2020.89146

[50] Han, D.D., Liu, X.M., Cui, Y.D., *et al.* (2014) Simultaneous Picosecond and Femtosecond Solitons Delivered from a Nanotube-Mode-Locked All-Fiber Laser. *Optics Letters*, **39**, 1565-1568. https://doi.org/10.1364/OL.39.001565

[51] Wei, Y., Li, B., Wei, X., Yu, Y. and Wong, K.K.Y. (2018) Ultrafast Spectral Dynamics of Dual-Color-Soliton Intracavity Collision in a Mode-Locked Fiber Laser. *Applied Physics Letters*, **112**, Article ID: 081104. https://doi.org/10.1063/1.5020821

[52] Sukhorukov, A., Neshev, D., Dreischuh, A., *et al.* (2008) Observation of Polychromatic Gap Solitons. *Optics Express*, **16**, 5991-5996.

https://doi.org/10.1364/OE.16.005991

[53] Feshchenko, V. and Feshchenko, G. (2020) Nonstationary CARS by Polaritons. *Journal of Applied Mathematics and Physics*, **9**, 2193-2204. https://doi.org/10.4236/jamp.2020.89146

[54] Strizhevskii, V.L. (1972) Theory of Stimulated Raman Scattering by Polaritons in Cubic and Uniaxial Crystals. *Zh. Eksp. Teor. Fiz.*, **35**, 760-766.

[55] Akhmanov, S.A. and Khokhlov, R.V. (1964) Problems of Nonlinear Optics.

[56] Harvey, J.D., Proctor, M.J. and Steed, C.A. (1988) 30 ps Cavity-Dumped Pulses from an Argon Laser. *Applied Physics Letters*, **52**, 688. https://doi.org/10.1063/1.99348

[57] Cheng, Y.C., Jin, C.Q., Gao, F., Wu, X.L., Zhong, W., Li, S.H. and Chu, P.K. (2009) Raman Scattering Study of Zinc-Blende and Wurtzite ZnS. *Journal of Applied Physics*,**106**, Article ID:123505. https://doi.org/10.1063/1.3270401